Online-Journals.org

iJOE International Journal of Online and Biomedical Engineering

iJOE | eISSN: 2626-8493 | Vol. 21 No. 13 (2025) | OPEN ACCESS

https://doi.org/10.3991/ijoe.v21i13.56605

PAPER

Discrete Neuroimaging Metrics for Identifying Structural Alterations in COVID-19-Related Brain Atrophy

Duniel Delgado-Castillo[1], Eduardo Barbará-Morales[2,3], Nidiyare Hevia-Montiel[4], Fernando Arámbula-Cosío[4], Didier Torres-Guzmán[1] (✉)

[1]National Autonomous University of Mexico, Ciudad de México, Mexico

[2]Universidad Anáhuac Mayab, Mérida, Yucatán, Mexico

[3]Universidad Politécnica de Yucatán, Mérida, Yucatán, Mexico

[4]Universidad Nacional Autónoma de México, Mérida, Yucatán, Mexico

didier.torres@unam.mx

ABSTRACT

Several studies have evidenced the effects of SARS-CoV-2 on the central nervous system. In some cases, neurological symptoms have manifested with medium- to long-term persistence, suggesting the presence of brain damage. Our objective is to evaluate discrete tortuosity (T_d) and discrete compactness (C_d) as potential imaging biomarkers to quantify atrophic alterations caused by the pathology in various cerebral structures. T1-weighted magnetic resonance images were utilized to compare brain morphologies between 316 recovered COVID-19 patients and 316 matched controls, all over 60 years old. Morphological biomarkers, including T_d, C_d, volume (V), and mean cortical thickness (M_{ct}), were then applied to assess structural changes in different brain regions. Compared to controls, results for the COVID-19 patients showed a statistically significant ($p < 0.05$) increase in T_d and a decrease in C_d within the left cerebral cortex, left temporal lobe, left lateral orbitofrontal cortex, and left superior temporal gyrus, while the V and M_{ct} metrics showed non-significant reductions in the same structures. A statistically significant decrease in M_{ct} was observed in the right frontal lobe and left inferior temporal gyrus. Our results showed an increase in cortical gray matter atrophy in COVID-19 patients, potentially linked to neurodegenerative processes, with a greater prevalence in the left hemisphere. These findings suggest that T_d and C_d are sensitive metrics for detecting subtle atrophic changes and may complement traditional measures, which could enhance the assessment of SARS-CoV-2-associated brain alterations.

KEYWORDS

COVID-19, discrete tortuosity (T_d), discrete compactness (C_d), morphological biomarkers

1 INTRODUCTION

The COVID-19 pandemic experienced in recent years had a significant negative impact on human health worldwide [1], [2]. Although the pandemic has ended, the damage inflicted on the human body has not yet been fully elucidated [3]. Due to this uncertainty and the persistence of sequelae in some infected individuals,

Delgado-Castillo, D., Barbará-Morales, E., Hevia-Montiel, N., Arámbula-Cosío, F., Torres-Guzmán, D. (2025). Discrete Neuroimaging Metrics for Identifying Structural Alterations in COVID-19-Related Brain Atrophy. *International Journal of Online and Biomedical Engineering (iJOE)*, 21(13), pp. 97–112. https://doi.org/10.3991/ijoe.v21i13.56605

Article submitted 2025-05-13. Revision uploaded 2025-08-21. Final acceptance 2025-08-22.

the scientific and medical community continues to investigate the long-term effects of the SARS-CoV-2, also referred to as long COVID [4], [5], with implications that extend beyond health into educational and social domains [6], [7]. This condition can manifest through various symptoms, such as breathing difficulties, anosmia, palpitations, poor concentration, depression, anxiety, and sleep disruptions, among others, which may persist for months after the infection [8]. Studies conducted in this regard suggest that COVID-19 is not limited to respiratory involvement. In addition, it has significant implications for the central nervous system [9], [10], [11]. This has led to investigations of the brain, where alterations in structure or function have been detected as a result of direct viral invasion or neuro-inflammatory processes that induce neuronal death [12], [13], [14], [15]. Evidence of neuronal damage has been corroborated by post-mortem analysis of brain tissue samples [16], [17].

To study alterations in cerebral morphology, various biomarkers derived from neuroimaging have been explored [12], [14], [15]. Several investigations in this regard have reported abnormalities in brain anatomy. However, these modifications can be subtle and, in some cases, contradictory [18]. Although most studies report a decrease in gray matter *V* in infected individuals [19], [20], [21], other researchers have observed an increase in both cortical and subcortical structures [22]. It is also worth noting that, even when some studies agree on affected regions, there is a variety of reported areas [12], [14], [23].

As part of the neuroimaging biomarkers reported in the scientific literature for quantifying atrophic damage, Perlaki et al. [18] conducted a study involving 38 young adult subjects who contracted COVID-19 and 37 healthy subjects. The authors reported a statistically significant reduction in M_{ct} and subcortical gray matter *V* in patients who recovered from a mild course of COVID-19. Additionally, segmentation of the olfactory bulb was performed with the assistance of a specialist, revealing a decrease in the *V* of its right section. The small sample size, the participants' youth, and the requirement for a longitudinal investigation are some of the study's limitations [18].

Romero et al. [20] combined cerebral morphological biomarkers, neuropsychological tests, and inflammatory and coagulation biomarkers to elucidate the impacts of COVID-19 on cerebral structure and function. In the investigation, 39 recovered cases were compared with 39 control subjects. Patterns of cortical thickness deterioration between groups were identified through cluster analysis and principal component analysis. The results indicate persistent alterations in cerebral structures, which may be related to prolonged neurological symptoms following COVID-19 recovery. The researchers highlight various limitations in their work, such as the limited number of participants, the lack of cognitive assessments prior to infection, and the absence of initial magnetic resonance imaging (MRI) scans during the disease's early stages.

Other authors employed voxel-based morphometry, combined with regional homogeneity and the amplitude of low-frequency fluctuations, to examine structural and functional changes in 21 young participants affected by SARS-CoV-2. Jin et al. [15] conducted a longitudinal investigation, reporting functional alterations as well as a reduction in the *V* of left thalamic gray matter. They also mentioned some limits to their study, like the small number of participants and that it only included female patients.

A longitudinal study reported by Douaud et al. [12] compared a group of 401 COVID-19 patients with 384 control subjects. Some of the metrics employed included regional gray matter *V*, cortical surface area, cortical *V*, and local cortical thickness. The study highlighted changes linked to SARS-CoV-2 infection, particularly

involving significant atrophy and heightened tissue alteration in cortical regions associated with the primary olfactory cortex. The COVID group exhibited a greater decrease in mean cortical thickness, reaching statistical significance in the left lateral orbitofrontal cortex according to the statistical model applied by the authors. A decrease in tissue contrast was observed in the orbitofrontal cortex and parahippocampal gyrus, along with reductions in overall and local brain *V*. A key limitation of the research is the absence of data on the severity of COVID-19 infection and the associated symptoms.

Deuter et al. [14] examined structural brain changes induced by SARS-CoV-2 and their impact on executive function. This study included 16 patients with acute COVID-19, 21 recovered patients, and 13 healthy participants. Voxel-based morphometry was employed to analyze gray matter, while probabilistic tractography assessed white matter tracts. COVID-19 patients showed alterations in gray and white matter, mainly in the temporal and frontal lobes, cerebellum, and basal ganglia, with greater effects on the left hemisphere. Acute patients exhibited significant gray matter reduction in the left fusiform and inferior temporal gyrus, hippocampus, parahippocampal gyrus, and both cerebellar hemispheres. The authors acknowledged several limitations in the study, including different MRI scanners, small sample size, lack of longitudinal data, and exclusion of patients with preexisting brain pathologies.

Previous studies regarding post-COVID-19 cerebral morphological alterations have shown variable and occasionally contradictory results in both the specific affected regions and the extent of cerebral damage. These inconsistencies are likely influenced by the heterogeneity of study populations in terms of disease severity, comorbidities, and age. We propose the use of the discrete tortuosity (T_d) and compactness (C_d) metrics as an alternative approach to these studies. By focusing on the geometric complexity of cerebral structures, these metrics may reveal subtle changes that traditional volumetric analysis might overlook, enabling a more detailed characterization of morphological alterations. These metrics have already demonstrated sensitivity as indicators of other cerebral pathologies associated with morphological changes. Furthermore, T_d and C_d may provide a detailed characterization of the persistent effects of the infection associated with changes in cerebral morphology. Finally, this study aims to contribute to future research on neuroimaging biomarkers related to morphological changes induced by SARS-CoV-2.

2 MATERIALS AND METHODS

2.1 Dataset overview

The UK Biobank (UKBB) [24] provided the neuroimaging data analyzed in this study to assess the effects of SARS-CoV-2 on cerebral morphology. Multimodal brain imaging was collected as part of the UKBB initiative, adhering to standardized protocols and rigorous quality assurance procedures [25], [26].

To conduct this study, 316 individuals who tested positive for COVID-19 were selected and matched with 316 control participants based on specific criteria. The COVID group consisted of individuals whose positivity was confirmed through valid tests (see details in UKBB showcase data field 41001). Control participants were identified as those with negative test results or no documented evidence of SARS-CoV-2 in their medical history. Both groups included only participants over 60 years old. Matching was performed based on factors such as age, sex, and ethnic group,

as described in UKBB showcase data-field 41000. Authorization to utilize the UKBB data was granted through the established procedure. Table 1 provides the demographic details for both groups.

Table 1. Summary of the included participants' demographic information

	COVID	Control	*p*-Value
Number of participants	316	316	–
Sex (male/female)	148 (46.8%)/168 (53.2%)	148 (46.8%)/168 (53.2%)	1.00[a]
Diagnosed diabetes	20 (6.3%)	12 (3.8%)	0.21[a]
Age (mean ± standard deviation)	67.73 ± 5.03	67.71 ± 4.98	0.99[b]
Blood pressure – diastolic component (mmHg)	80.36 ± 10.76	79.46 ± 10.34	0.25[c]
Blood pressure – systolic component (mmHg)	148.0 ± 21.4	147.6 ± 21.1	0.56[c]
Ethnicity (white/non-white)	272 (86.1%)/44 (13.9%)	273 (86.4%)/43 (13.6%)	1.00[a]
Body mass index (kg/m^2)	26.36 ± 4.48	26.08 ± 4.40	0.55[c]
Weight (kg)	74.56 ± 14.05	74.04 ± 14.45	0.63[c]
Waist/hip ratio	0.91 ± 0.09	0.89 ± 0.09	0.14[c]

Notes: [a]χ^2 tests, [b]two-sample Kolmogorov–Smirnov tests, [c]Mann–Whitney U-tests.

2.2 MRI acquisition

All images used in this study were acquired under the detailed acquisition protocol of the UKBB [27]. The imaging system is a Siemens 3T MRI scanner with a 32-channel RF head coil. T1-weighted structural MRI is obtained with a straight sagittal orientation, featuring a resolution of 1×1×1 mm and a field-of-view compatible with a matrix size of 208×256×256. The 3D-Magnetization Prepared Rapid Gradient Echo technique was employed for image acquisition. The protocol also included prescan normalization, an in-plane acceleration factor of 2, and timing parameters set at TI/TR = 880/2000 ms.

2.3 MRI structural analysis

T1-weighted MRI images were processed and segmented using FreeSurfer 6.0, a well-documented neuroimaging suite available through its official website (https://surfer.nmr.mgh.harvard.edu). To compare brain structures between the COVID and control groups, the Desikan–Killiany–Tourville (DKT) neuroanatomical labeling atlas [28] was employed. Figure 1a presents an example of processed images, displaying a T1-weighted MRI with intensity normalization and the delineated segmentation of the superior temporal cortex obtained using the DKT parcellation. This parcellation is represented as a discrete three-dimensional (3D) matrix of labels corresponding to each brain structure. Figure 1b presents both hemispheres of the superior temporal gyrus, clearly illustrating the discrete structural representation of anatomical information. These anatomical substructures, organized as 3D voxel arrays, will be

employed to efficiently quantify, via discrete biomarkers, the atrophic changes associated with the pathology under investigation.

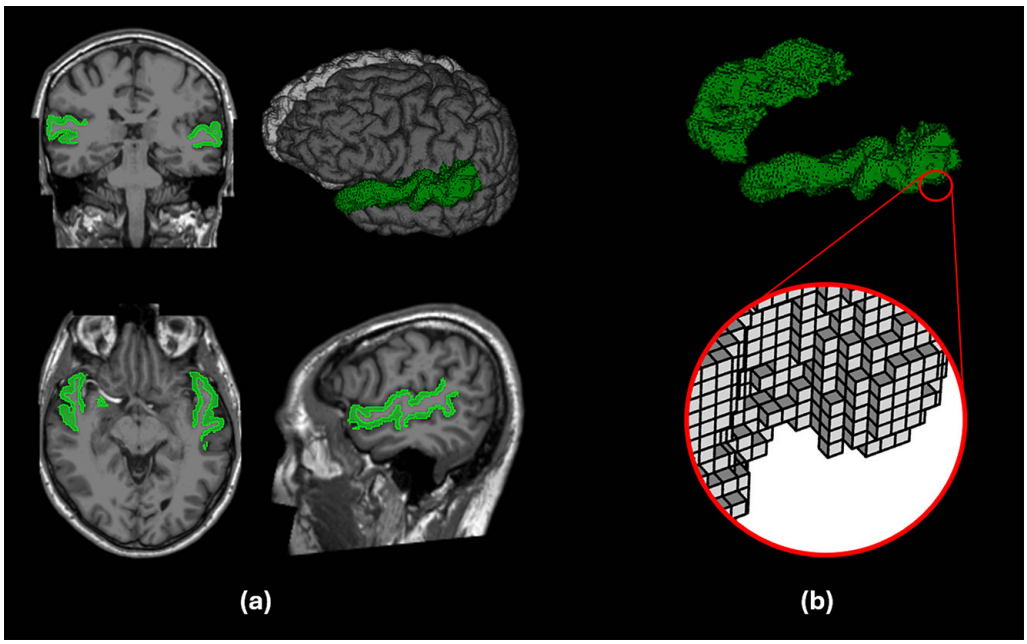

Fig. 1. (a) Superior temporal gyrus in a T1-weighted MRI, as used in this study. **(b)** Illustration of the cortical surface before the metric extraction process

Source: The image was obtained from the UKBB example files.

2.4 Metrics

Discrete tortuosity. Tortuosity is an inherent characteristic of 2D and 3D curves, offering valuable information regarding variations in their slope or curvature. This metric has been employed across multiple disciplines, playing a critical role in computational analysis and pattern recognition. Its application has been documented in several contexts, including retinal vessel conditions, Alzheimer's disease, and brain tumors [29], [30], [31], [32], [33].

Considering these antecedents, this study proposes the use of the T_d measure introduced by Bribiesca [34]. This metric is effective for quantifying 3D discretized objects composed of n voxels connected by their faces, thereby applicable to segmented MRI data. T_d captures the deviation of a structure from an ideal straight or flat configuration, providing insights into its geometric complexity. In neuroimaging, higher tortuosity may reflect pathological alterations in cortical and subcortical structures, making this metric a valuable complement to conventional volumetric indices. To introduce this T_d measure for 3D voxel arrays, several concepts and definitions will be outlined below.

To begin, we consider a 3D matrix composed of n voxels, where each voxel is assumed to have a length, width, and depth of 1. The contact surface area (A_c) of an object formed by n voxels connected through their faces is calculated by summing the areas of the contact surfaces shared between adjacent voxels. Figures 2a and c illustrate the contact surfaces in voxel arrangements that are connected to each other. Within the same 3D object, we can quantify the visible external faces of the voxels, referred to as the enveloping surface area (A), as demonstrated in Figures 2b and d.

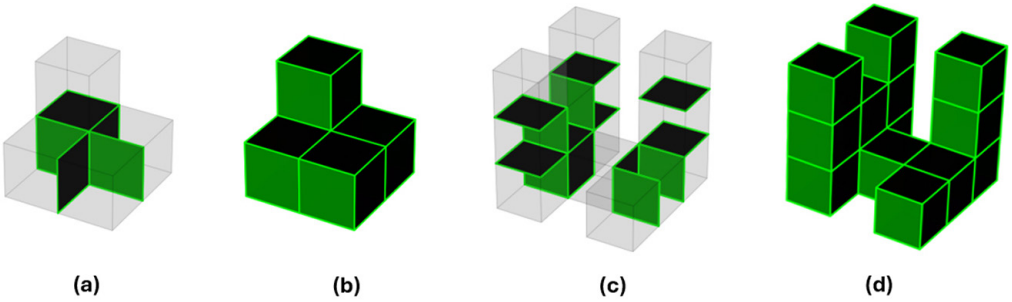

Fig. 2. Contact surface area (A_c) and enclosing surface area (A) for voxel-based objects of different sizes ($n = 5$ and $n = 14$): **(a)** $A_c = 5$; **(b)** $A = 20$; **(c)** $A_c = 15$; **(d)** $A = 54$

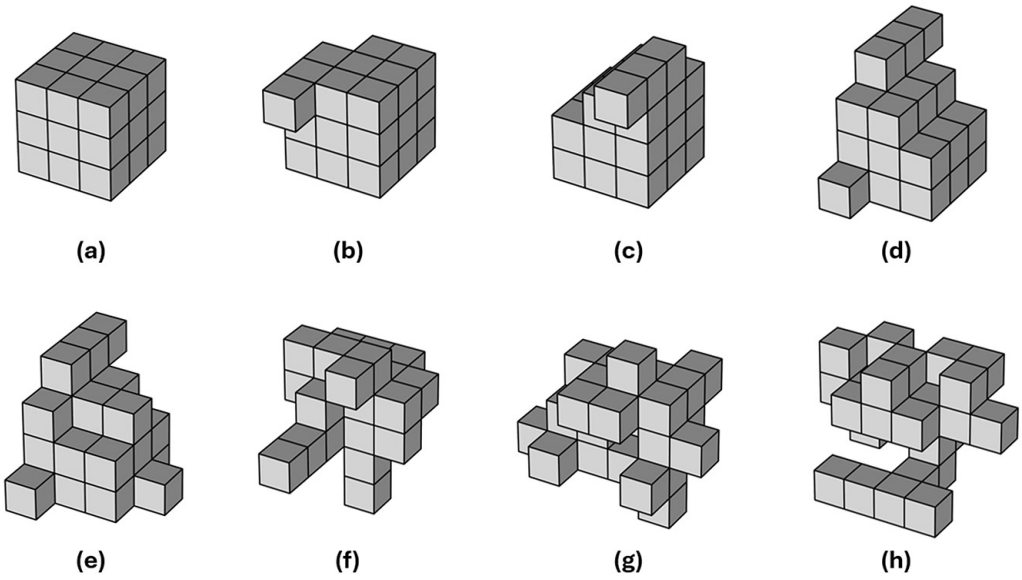

Fig. 3. Voxel-based objects ($n = 27$) illustrate variations in A_c contact surface area and T_d discrete tortuosity: **(a)** $A_c = 54$, $T_d = 0$; **(b)** $A_c = 52$, $T_d = 0.07142$; **(c)** $A_c = 50$, $T_d = 0.14285$; **(d)** $A_c = 48$, $T_d = 0.21428$; **(e)** $A_c = 45$, $T_d = 0.32142$; **(f)** $A_c = 40$, $T_d = 0.5$; **(g)** $A_c = 35$, $T_d = 0.67857$; **(h)** $A_c = 28$, $T_d = 0.92857$

The relationship between both areas is defined by Bribiesca in [35] and is expressed by equation (1), where a represents the A_c between voxels (a = 1 for 1×1×1 voxels) and n corresponds to the number of voxels.

$$A = 6an - 2A_c \tag{1}$$

In a 3D object consisting of n voxels connected by their faces, the minimum enveloping area (A_{min}) and the maximum enveloping area (A_{max}) are defined by equations (2) and (3), respectively [34]. These equations allow for the quantification of the boundary characteristics of the voxelized structures, offering insights into their geometric properties.

$$A_{min} = 6\,(\sqrt[3]{n})^2 \tag{2}$$

$$A_{max} = 4n + 2 \tag{3}$$

Once these parameters are obtained, the T_d measure proposed by Bribiesca [34] can be calculated. This metric can be expressed as a function of the contact area and the minimum (A_{min}) and maximum (A_{max}) enveloping areas, as defined in equation (4).

Figures 3a–h present the calculated T_d values for the structure consisting of 27 voxels, illustrating how this metric varies as the structure undergoes deformation.

$$T_d = \frac{A - A_{min}}{A_{max} - A_{min}} \tag{4}$$

The proposed measure T_d is invariant to translation, rotation, and scaling. Furthermore, it is maintained at different resolutions and can be applied to structures with cavities and passages [34]. It is scaled to a continuous range between 0 and 1, enabling enhanced object classification. These features make T_d an effective metric for quantifying irregular surfaces, such as brain structures, which is particularly advantageous for identifying atrophic changes caused by COVID-19 in the brain.

Discrete compactness. Compactness describes how much mass is packed into an object compared to its size and surface, with a sphere representing the optimal shape. This metric has been applied effectively in various fields, including medicine [36]. However, classical compactness measures rely heavily on the enveloping surface, making them particularly vulnerable to noise. In practical scenarios, objects often have noisy surfaces, which influences their compactness measurements. Therefore, the C_d measure proposed in [35] will be utilized. This measure largely depends on the total contact surface areas of voxels connected by their faces for 3D objects, as defined by equation (5):

$$C_d = \frac{n - \frac{A}{6}}{n - (\sqrt[3]{n})^2} \tag{5}$$

where n represents the voxel count and A is the enveloping area, as illustrated in Figures 2b and d. With this proposal, it is possible to calculate measures for any type of object using a simple equation, including porous and fragmented objects, while maintaining invariance to translation, rotation, and scaling. This metric varies linearly and discretely between 0 and 1, reaching its maximum value in the digital cube. This represents an advantage in the computational process of analyzing and classifying shapes, which can be particularly useful for quantifying changes in brain structures. In neuroimaging, C_d serves as a complementary descriptor to volume and cortical thickness, capturing the degree to which brain structures deviate from compact configurations. A reduction in compactness may reflect cortical or subcortical atrophy.

Volume. Volume is an essential attribute used to describe 3D objects. In 3D digital images, this spatial information is represented in an array of discrete voxels, where each voxel contains information about a small portion of the 3D space, similar to how a pixel functions in 2D images. This matrix enables precise representation and analysis of the object within this volumetric space. In this study, given that the MRI scan was acquired with an isotropic resolution of 1×1×1 mm, the volume to be quantified is equivalent to the sum of all n voxels included in the region under analysis.

Mean cortical thickness. Cortical thickness is a commonly used metric to quantify changes in the gray matter of the cerebral cortex [12], [18]. It represents the distance from the white surface to the pial surface, as shown in Figure 4. In this study, the M_{ct} was obtained for the cortical structure based on the DKT parcellation of FreeSurfer version 6.0. Additionally, M_{ct} was calculated for the cerebral cortex of each hemisphere and the analyzed lobes to measure changes in this metric caused by the studied pathology.

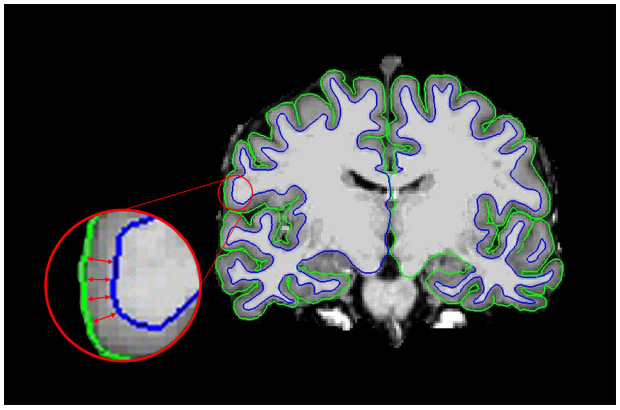

Fig. 4. Representation of cortical thickness in the coronal plane from a T1-weighted MRI scan

2.5 Study design

To evaluate COVID-19's impact on cerebral anatomy using the proposed metrics, the T1-weighted MRI scans from the COVID and control groups were segmented according to the DKT parcellation using FreeSurfer. For the region represented in a 3D matrix obtained from the segmentation and parcellation process, T_d, C_d, V, and M_{ct} were calculated. To specifically evaluate the performance of T_d and C_d, this study proposes quantifying brain structures commonly reported to exhibit alterations associated with COVID-19 [12], [14], [18] and vulnerability due to viral propagation within the brain [12], [13]. Under these assumptions, cortical gray matter in both hemispheres, as well as the frontal and temporal lobes, was assessed. Based on prior exploratory analyses, substructures of the left temporal lobe (including the fusiform gyrus, middle temporal gyrus, inferior temporal gyrus, parahippocampal gyrus, transverse temporal gyrus, and superior temporal gyrus) were further analyzed. Additional structure frequently associated with reported alterations, such as the lateral orbitofrontal cortex, was evaluated [23], [37]. All data processing, models, and algorithms used for quantifying these metrics were implemented in Python on the Research Analysis Platform (RAP). Once these metrics were obtained, a statistical analysis was conducted to compare the two groups, providing insights into the potential morphological alterations in the brain due to COVID-19.

2.6 Statistical analysis

Baseline group comparisons were conducted using statistical tests selected according to the scale of measurement and distributional properties of each variable. For age, the nonparametric Kolmogorov–Smirnov test for two samples was applied. Categorical variables, including diagnosed diabetes, ethnicity, and sex, were evaluated with χ^2 tests, which assess differences in the distribution of frequencies across groups. Continuous variables that are frequently non-normally distributed, such as weight, waist/hip ratio, body mass index, and blood pressure components, were compared using Mann–Whitney U-tests, which do not rely on normality assumptions and are appropriate for ordinal or skewed data. To examine morphometric differences between the COVID and control groups, either Mann–Whitney U-tests or independent-samples t-tests were applied, depending on whether the Shapiro–Wilk test supported the assumption of normality. Statistical significance was determined

using a *p*-value threshold of less than 0.05. The detailed statistical results obtained from these analyses are presented in the following sections.

3 RESULTS

After applying the proposed metrics, the results obtained in this study revealed anatomical differences in brain structures between COVID and control subjects. Statistical comparisons of morphometric biomarkers in the evaluated regions are presented in Table 2. Significant changes in T_d and C_d were observed in the left cerebral cortex, left temporal lobe, left superior temporal gyrus, and left transverse temporal gyrus. Additionally, T_d was significantly affected in the left lateral orbitofrontal cortex. Statistically significant differences in M_{ct} were found in the right temporal lobe and the left inferior temporal gyrus.

Table 2. Statistical comparison of morphological biomarkers between COVID and control groups

	Discrete Tortuosity	Discrete Compactness	Volume	Mean Cortical Thickness
Right cerebral cortex				
Left cerebral cortex	*	*		
Right frontal lobe				
Left frontal lobe				
Right temporal lobe				*
Left temporal lobe	*	*		
Fusiform gyrus				
Inferior temporal gyrus				*
Middle temporal gyrus				
Parahippocampal gyrus				
Superior temporal gyrus	*	*		
Transverse temporal gyrus	*	*		
Right lateral orbitofrontal cortex				
Left lateral orbitofrontal cortex	*			

Notes: *Indicates statistical significance with Mann–Whitney U-tests or independent-samples t-tests ($p < 0.05$).

In the following figures, we present analyses focused on the left temporal lobe, the left lateral cerebral cortex, and the left lateral orbitofrontal cortex, selected for their relevance to COVID-19. Previous studies [12], [14], [18] have frequently highlighted that these regions are affected by infection, potentially mediated by the olfactory pathway and neuro-inflammatory processes. Furthermore, these areas are critical for cognitive and emotional functions, which may be disrupted in post-COVID patients [20], [23]. Notably, these structures exhibited the most significant differences in T_d and C_d metrics ($p < 0.05$), supporting their inclusion in graphical representations. Figure 5 presents a detailed analysis of the metrics evaluated in the left cerebral cortex. The box plots demonstrate a significant increase in T_d ($p = 0.0283$), along with a significant decrease in C_d ($p = 0.0288$), in the COVID group relative to the control group. Additionally, the graphs show a decrease in V and M_{ct}, although these changes did not reach statistical significance.

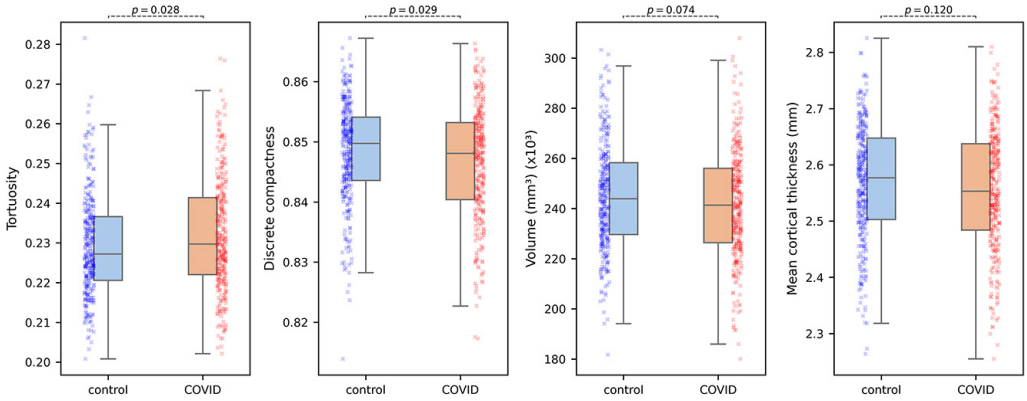

Fig. 5. Statistical analysis of T_d, C_d, volume, and mean cortical thickness for the left cerebral cortex

A comparable pattern is observed in the biomarkers evaluated in the left temporal lobe. Figure 6 displays a trend toward a decrease in V and M_{ct}, in addition to a statistically significant increase in T_d ($p = 0.0364$) along with a significant reduction in C_d ($p = 0.0373$). The results of the metrics applied to the left lateral orbitofrontal cortex are shown in Figure 7. These illustrate that V, C_d, and M_{ct} are lower in the COVID group. In this case, the comparisons reached statistical significance only for the T_d metric ($p = 0.0493$).

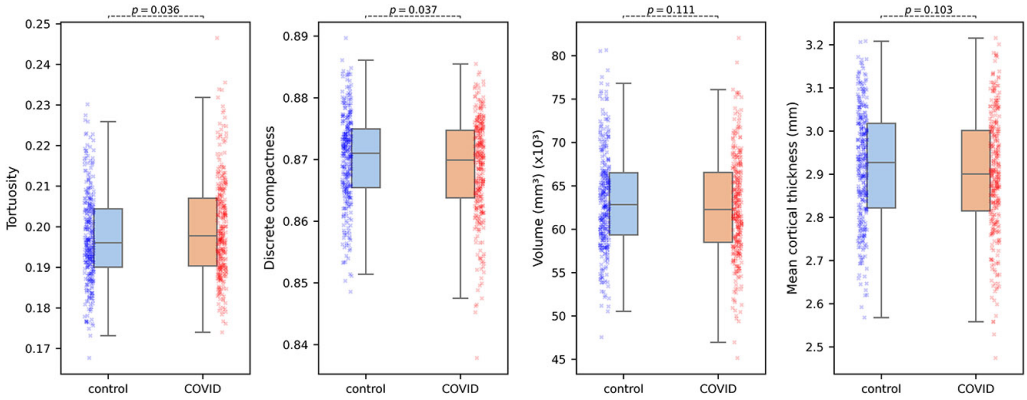

Fig. 6. Statistical analysis of T_d, C_d, volume, and mean cortical thickness for left temporal lobe

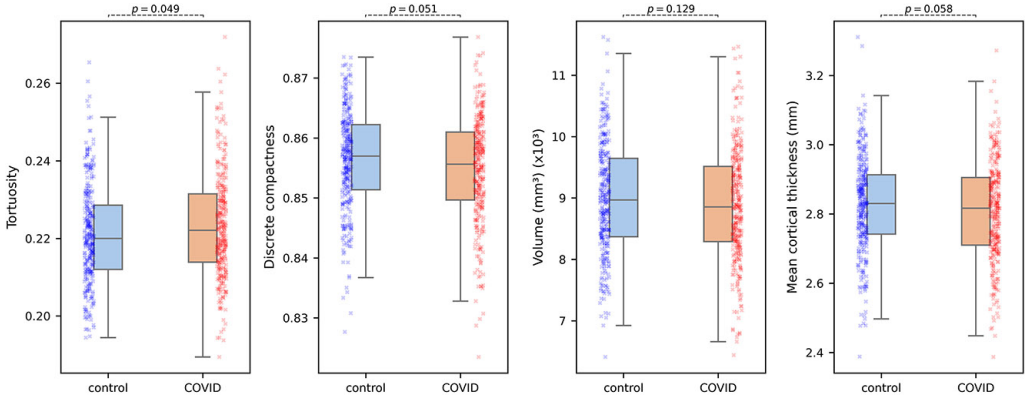

Fig. 7. Statistical analysis of T_d, C_d , volume, and mean cortical thickness for the left lateral orbitofrontal cortex

4 DISCUSSION

This study examined structural brain abnormalities in an adult population affected by COVID-19, evaluating structural biomarkers such as T_d, C_d, V and M_{ct}. The evaluation of the proposed metrics within the gray matter revealed an increase in T_d and a reduction in C_d, mean cortical thickness, and volume when comparing COVID-19 subjects to controls. This study's results are consistent with previous evidence reported for volume and mean cortical thickness [12], [18]. For instance, Perlaki et al. [18] observed decreased olfactory bulb volume, subcortical gray matter volume, and mean cortical thickness when comparing COVID-19 subjects with controls. The authors also noted that, in cortical structures, statistically significant changes were observed in the right lateral orbitofrontal cortex. Our findings further highlight this gray matter deterioration in COVID-19 cases through morphometric changes evident in the measures of T_d and C_d. As illustrated in Figure 5, for the left cerebral cortex, T_d exhibited a statistically significant increase ($p = 0.0283$), and C_d a statistically significant reduction ($p = 0.0288$), accompanied by non-significant reductions in V ($p = 0.0736$) and M_{ct} ($p = 0.1232$). Similarly, for the left temporal lobe (Figure 6), the biomarkers revealed statistically significant changes in T_d ($p = 0.03643$) and C_d ($p = 0.03738$), along with non-significant reductions in V ($p = 0.1109$) and M_{ct} ($p = 0.1032$). These results suggest that T_d and C_d are more sensitive metrics for detecting cortical alterations, as they exhibit greater statistical significance and faster responses to morphological changes compared to volume and mean cortical thickness, which show nonsignificant differences in this analysis.

Those alterations found in the gray matter also line up with Deuter et al. [14] and Douaud et al.'s [12] reports. Deuter et al. [14] reported significant differences in gray matter between acute cases and recovered individuals in substructures of the temporal lobe (left fusiform gyrus, left inferior temporal gyrus, and left parahippocampal gyrus), including the left hippocampus and both hemispheres of the cerebellum. The researchers mentioned a greater incidence in the left hemisphere. This trend is consistent with our findings, more prominently evidenced by the biomarkers T_d and C_d. The same conclusion regarding a greater tendency for alterations in the left hemisphere was noted by Douaud et al. [12]. They also reported, among their findings, a global reduction in brain volume in COVID-19 patients, alongside an increase in cerebrospinal fluid. They also reported a significant reduction in the left lateral orbitofrontal cortex. In our analysis of this specific substructure of the orbitofrontal cortex, we confirmed its deterioration, as illustrated in Figure 7. In this region, T_d exhibited a statistically significant increase ($p = 0.04933$), while non-significant decreases were observed for C_d ($p = 0.05143$), V ($p = 0.1287$), and M_{ct} ($p = 0.05791$). Note that, although reductions in volume and mean cortical thickness were observed, the statistically significant change in T_d suggests that this metric is more sensitive for quantifying the deterioration of this substructure. Additionally, statistically significant alterations in C_d and T_d were identified in the left superior temporal gyrus and the left transverse temporal gyrus, as shown in Table 2. Special attention should be given to the morphological changes detected in these structures of the temporal lobe, as the proposed metrics reveal changes that are not yet significantly apparent in volume or mean cortical thickness.

The findings obtained from the analyzed structures, using the metrics of T_d and C_d, suggest that these could be used as biomarkers for quantifying brain atrophy in patients affected by COVID-19. These metrics identified statistically significant differences in several analyzed structures more frequently than changes in volume and mean cortical thickness, demonstrating their sensitivity in detecting morphological variations. T_d and C_d have also demonstrated encouraging results in measuring structural changes in other pathologies, such as Alzheimer's disease [29], [38].

The atrophic changes reflected by the biomarkers proposed in our study could, according to the scientific literature, be associated with pathophysiological processes of neuronal death that result in tissue damage. Two main hypotheses regarding neuronal death have been proposed. The first hypothesis suggests a direct relationship with the virus [39], [40], [41], while the second relates to neuro-inflammatory effects induced by the infection [42], [43]. Crunfli et al. [44] described a model where SARS-CoV-2 infects astrocytes through interaction with Neuropilin-1 and subsequently affects neuronal function and viability. Another article published by Kong et al. [45] revealed that neuronal death in the scenario of SARS-CoV-2 infection is not primarily due to direct viral invasion but rather to inflammation induced by the infection. Their research suggests that the neurons that die are mostly cells not directly infected by the virus but neighboring cells affected by the hostile environment created by astrocyte infection [45].

The findings of this study suggest that COVID-19 infection may induce structural alterations in cortical gray matter, with a notable impact on regions of the temporal and frontal lobes and an accentuation of atrophic changes in the left hemisphere. T_d and C_d in this case study demonstrate their advantages in diagnosing brain atrophy, suggesting their potential use as biomarkers for monitoring this pathology. It is also important to highlight that these metrics are invariant to scaling, rotation, and image resolution. Additionally, they are normalized within a continuous range from 0 to 1, making them computationally efficient and easy to implement [34]. These characteristics enhance their potential applicability in clinical practice as feasible imaging biomarkers for quantifying this condition. It is important to acknowledge that this study has several limitations that should be considered when interpreting the findings. First, information regarding the severity of COVID-19 infection and the specific symptoms associated with central nervous system alterations was not available. These factors may influence brain abnormalities, particularly given the heterogeneous clinical manifestations of SARS-CoV-2 infection. Second, the absence of cognitive and neuropsychological assessments limits the ability to establish direct correlations between the observed morphological changes and potential functional impairments or clinical outcomes. Finally, the analysis did not include additional neuroimaging modalities, such as diffusion tractography or functional MRI, which could have complemented the structural metrics proposed in this investigation.

5 CONCLUSION

The discrete morphological metrics of tortuosity and compactness revealed significant differences when comparing the cortical structures of COVID-19 and control subjects. Significant changes were identified in the left cerebral cortex, left temporal lobe, left lateral orbitofrontal cortex, left superior temporal gyrus, and left transverse temporal gyrus, suggesting a pronounced pattern of deterioration in the left hemisphere. These findings underscore these metrics' sensitivity to atrophic changes in brain morphology. The results suggest that T_d and C_d could be considered as imaging biomarkers for assessing SARS-CoV-2-induced morphological deterioration in the brain.

6 ETHICS DECLARATIONS

The data analyzed in this investigation were obtained from the UK Biobank, which operates under the approval of the North West Multi-Centre Research Ethics Committee (MREC), in which all participants provided written informed consent.

All procedures were conducted in accordance with UK Biobank's ethical and governance framework (https://www.ukbiobank.ac.uk/ethics) and under the terms of access granted for this project (Application Number: 212767).

7 DATA AVAILABILITY

The source data can be accessed through a formal procedure with UK Biobank.

8 CONFLICT OF INTEREST

The authors disclose no conflicts.

9 REFERENCES

[1] WHO COVID-19 dashboard, "COVID-19 cases, World," 2024. [Online]. Available: https://data.who.int/dashboards/covid19/cases [Accessed: Feb. 7, 2025].

[2] A. A. Rabaan *et al.*, "SARS-CoV-2 infection and multi-organ system damage: A review," *Biomol. Biomed.*, vol. 23, no. 1, pp. 37–52, 2023. https://doi.org/10.17305/bjbms.2022.7762

[3] Z. Al-Aly and C. J. Rosen, "Long covid and impaired cognition—More evidence and more work to do," *N. Engl. J. Med.*, vol. 390, no. 9, pp. 858–860, 2024. https://doi.org/10.1056/NEJMe2400189

[4] S. Lopez-Leon *et al.*, "More than 50 long-term effects of COVID-19: A systematic review and meta-analysis," *MedRxiv Prepr. Serv. Health Sci.*, 2021. https://doi.org/10.1101/2021.01.27.21250617

[5] World Health Organization, "Post COVID-19 condition (Long COVID)," 2022. [Online]. Available: https://www.who.int/europe/news-room/fact-sheets/item/post-covid-19-condition [Accessed: Feb. 7, 2025].

[6] P. D. McCray and N. S. S. Clair, "Overview of preliminary study findings: Evaluating the efficacy of the comprehensive institutional model in a post-COVID-19 hyflex higher education setting," *Int. J. Adv. Corp. Learn. (IJAC),* vol. 18, no. 2, pp. 51–59, 2025. https://doi.org/10.3991/ijac.v18i2.52573

[7] M. Peiris, "Unravelling technology acceptance: Lessons learnt from teacher's experience during COVID-19 for post-pandemic systemic education," *Int. J. Emerg. Technol. Learn. (IJET)*, vol. 19, no. 7, pp. 59–80, 2024. https://doi.org/10.3991/ijet.v19i07.51367

[8] A. Natarajan *et al.*, "A systematic review and meta-analysis of long COVID symptoms," *Syst. Rev.*, vol. 12, no. 1, p. 88, 2023. https://doi.org/10.1186/s13643-023-02250-0

[9] A.-C. Granholm, "Long-term effects of SARS-CoV-2 in the brain: Clinical consequences and molecular mechanisms," *J. Clin. Med.*, vol. 12, no. 9, 2023. https://doi.org/10.3390/jcm12093190

[10] A. B. Reiss *et al.*, "Long COVID, the brain, nerves, and cognitive function," *Neurol. Int.*, vol. 15, no. 3, pp. 821–841, 2023. https://doi.org/10.3390/neurolint15030052

[11] S. Spudich and A. Nath, "Nervous system consequences of COVID-19," *Science*, vol. 375, no. 6578, pp. 267–269, 2022. https://doi.org/10.1126/science.abm2052

[12] G. Douaud *et al.*, "SARS-CoV-2 is associated with changes in brain structure in UK Biobank," *Nature*, vol. 604, no. 7907, pp. 697–707, 2022. https://doi.org/10.1038/s41586-022-04569-5

[13] S. G. Kandemirli, A. Altundag, D. Yildirim, D. E. Tekcan Sanli, and O. Saatci, "Olfactory bulb MRI and paranasal sinus CT findings in persistent COVID-19 anosmia," *Acad. Radiol.*, vol. 28, no. 1, pp. 28–35, 2021. https://doi.org/10.1016/j.acra.2020.10.006

[14] D. Deuter *et al.*, "SARS-CoV2 evokes structural brain changes resulting in declined executive function," *PLoS ONE*, vol. 19, no. 3, p. e0298837, 2024. https://doi.org/10.1371/journal.pone.0298837

[15] P. Jin, F. Cui, M. Xu, Y. Ren, and L. Zhang, "Altered brain function and structure pre- and post- COVID-19 infection: A longitudinal study," *Neurol. Sci.,* vol. 45, no. 1, pp. 1–9, 2024. https://doi.org/10.1007/s10072-023-07236-3

[16] T. Wierzba-Bobrowicz *et al.*, "Neuropathological analysis of the brains of fifty-two patients with COVID-19," *Folia Neuropathol.*, vol. 59, no. 3, pp. 219–231, 2021. https://doi.org/10.5114/fn.2021.108829

[17] S. S. Mukerji and I. H. Solomon, "What can we learn from brain autopsies in COVID-19?" *Neurosci. Lett.*, vol. 742, p. 135528, 2021. https://doi.org/10.1016/j.neulet.2020.135528

[18] G. Perlaki *et al.*, "Gray matter changes following mild COVID-19: An MR morphometric study in healthy young people," *J. Magn. Reson. Imaging*, vol. 59, no. 6, pp. 2152–2161, 2024. https://doi.org/10.1002/jmri.28970

[19] S. Eliaçik and M. Büyükşireci, "Asymptomatic COVID-19 and structural changes in the brain," *Anatol. Curr. Med. J.*, vol. 6, no. 1, pp. 59–64, 2024. https://doi.org/10.38053/acmj.1386041

[20] A. O. Romero-Molina *et al.*, "SARS-CoV-2's brain impact: Revealing cortical and cerebellar differences via cluster analysis in COVID-19 recovered patients," *Neurol. Sci.,* vol. 45, no. 3, pp. 837–848, 2024. https://doi.org/10.1007/s10072-023-07266-x

[21] K. Duan *et al.*, "Alterations of frontal-temporal gray matter volume associate with clinical measures of older adults with COVID-19," *Neurobiol. Stress*, vol. 14, p. 100326, 2021. https://doi.org/10.1016/j.ynstr.2021.100326

[22] Y. Lu *et al.*, "Cerebral micro-structural changes in COVID-19 patients – An MRI-based 3-month follow-up study," *EClinicalMedicine*, vol. 25, p. 100484, 2020. https://doi.org/10.1016/j.eclinm.2020.100484

[23] A. A. Sharma, R. Nenert, A. M. Goodman, and J. P. Szaflarski, "Brain temperature and free water increases after mild COVID-19 infection," *Sci. Rep.*, vol. 14, p. 7450, 2024. https://doi.org/10.1038/s41598-024-57561-6

[24] UK Biobank, "Health research data for the world," 2025. [Online]. Available: https://www.ukbiobank.ac.uk [Accessed: Mar. 24, 2025].

[25] F. Alfaro-Almagro *et al.*, "Image processing and quality control for the first 10,000 brain imaging datasets from UK Biobank," *NeuroImage*, vol. 166, pp. 400–424, 2018. https://doi.org/10.1016/j.neuroimage.2017.10.034

[26] K. L. Miller *et al.*, "Multimodal population brain imaging in the UK Biobank prospective epidemiological study," *Nat. Neurosci.*, vol. 19, no. 11, pp. 1523–1536, 2016. https://doi.org/10.1038/nn.4393

[27] UK Biobank, "Brain imaging documentation," 2024. [Online]. Available: https://biobank.ndph.ox.ac.uk/showcase/ukb/docs/brain_mri.pdf

[28] A. Klein and J. Tourville, "101 labeled brain images and a consistent human cortical labeling protocol," *Front. Neurosci.*, vol. 6, 2012. https://doi.org/10.3389/fnins.2012.00171

[29] E. Barbará-Morales, J. Pérez-González, K. C. Rojas-Saavedra, and V. Medina-Bañuelos, "Evaluation of brain tortuosity measurement for the automatic multimodal classification of subjects with Alzheimer's disease," *Comput. Intell. Neurosci.*, vol. 2020, p. 4041832, 2020. https://doi.org/10.1155/2020/4041832

[30] W. E. Hart, M. Goldbaum, B. Côté, P. Kube, and M. R. Nelson, "Measurement and classification of retinal vascular tortuosity," *Int. J. Med. Inf.*, vol. 53, nos. 2–3, pp. 239–252, 1999. https://doi.org/10.1016/S1386-5056(98)00163-4

[31] E. Grisan, M. Foracchia, and A. Ruggeri, "A novel method for the automatic grading of retinal vessel tortuosity," *IEEE Trans. Med. Imaging*, vol. 27, no. 3, pp. 310–319, 2008. https://doi.org/10.1109/TMI.2007.904657

[32] N. Hevia-Montiel, E. Molino-Minero-Re, and A. J. Carrillo-Bermejo, "Discrete tortuosity as a morphometric measure in brain tumors," *Rev. Mex. Ing. Bioméd.*, vol. 38, no. 1, pp. 188–198, 2017. https://doi.org/10.17488/RMIB.38.1.13

[33] J. Perez-Gonzalez, L. Jiménez-Ángeles, K. Rojas Saavedra, E. Barbará Morales, and V. Medina-Bañuelos, "Mild cognitive impairment classification using combined structural and diffusion imaging biomarkers," *Phys. Med. Biol.*, vol. 66, no. 15, p. ac0e77, 2021. https://doi.org/10.1088/1361-6560/ac0e77

[34] E. Bribiesca, "A measure of tortuosity for enclosing surfaces of voxel-based objects," *SN Comput. Sci.*, vol. 2, no. 3, pp. 1–11, 2021. https://doi.org/10.1007/s42979-021-00565-0

[35] E. Bribiesca, "An easy measure of compactness for 2D and 3D shapes," *Pattern Recognit.*, vol. 41, no. 2, pp. 543–554, 2008. https://doi.org/10.1016/j.patcog.2007.06.029

[36] N. Hevia-Montiel, P. I. Rodriguez-Perez, P. J. Lamothe-Molina, A. Arellano-Reynoso, E. Bribiesca, and M. A. Alegria-Loyola, "Neuromorphometry of primary brain tumors by magnetic resonance imaging," *J. Med. Imaging Bellingham Wash*, vol. 2, no. 2, p. 024503, 2015. https://doi.org/10.1117/1.JMI.2.2.024503

[37] B. Kamasak *et al.*, "Effects of COVID-19 on brain and cerebellum: A voxel based morphometrical analysis," *Bratisl. Lek. Listy*, vol. 124, no. 6, pp. 442–448, 2023. https://doi.org/10.4149/BLL_2023_068

[38] M.-J. Mateos, E. Bribiesca, A. Guzmán-Arenas, W. Aguilar, and J. A. Marquez-Flores, "3D tortuosity computation as a shape descriptor and its application to brain structure analysis," *BMC Med. Imaging*, vol. 24, no. 1, p. 130, 2024. https://doi.org/10.1186/s12880-024-01312-6

[39] E. Song *et al.*, "Neuroinvasion of SARS-CoV-2 in human and mouse brain," *J. Exp. Med.*, vol. 218, no. 3, p. e20202135, 2021. https://doi.org/10.1084/jem.20202135

[40] S. R. Stein *et al.*, "SARS-CoV-2 infection and persistence in the human body and brain at autopsy," *Nature*, vol. 612, no. 7941, pp. 758–763, 2022. https://doi.org/10.1038/s41586-022-05542-y

[41] D. Wan *et al.*, "Neurological complications and infection mechanism of SARS-CoV-2," *Signal Transduct. Target. Ther.*, vol. 6, no. 1, pp. 1–16, 2021. https://doi.org/10.1038/s41392-021-00818-7

[42] E. A. Albornoz *et al.*, "SARS-CoV-2 drives NLRP3 inflammasome activation in human microglia through spike protein," *Mol. Psychiatry*, vol. 28, no. 7, pp. 2878–2893, 2023. https://doi.org/10.1038/s41380-022-01831-0

[43] I. H. C. H. M. Philippens *et al.*, "Brain inflammation and intracellular α-Synuclein aggregates in Macaques after SARS-CoV-2 infection," *Viruses*, vol. 14, no. 4, p. 776, 2022. https://doi.org/10.3390/v14040776

[44] F. Crunfli *et al.*, "Morphological, cellular, and molecular basis of brain infection in COVID-19 patients," *Proc. Natl. Acad. Sci. U. S. A.*, vol. 119, no. 35, p. e2200960119, 2022. https://doi.org/10.1073/pnas.2200960119

[45] W. Kong *et al.*, "Neuropilin-1 mediates SARS-CoV-2 infection of astrocytes in brain organoids, inducing inflammation leading to dysfunction and death of neurons," *mBio*, vol. 13, no. 6, p. e0230822, 2022. https://doi.org/10.1128/mbio.02308-22

10 AUTHORS

Duniel Delgado-Castillo is currently a PhD student at the National Autonomous University of Mexico. He obtained his Master's degree in Digital Signal and Image Processing from the Central University of Las Villas. His current research focuses on the computational processing of medical images, with a particular emphasis on brain imaging analysis.

Eduardo Barbará-Morales holds a Ph.D. in Biomedical Engineering (2019) with honors from UAM-I, Mexico. With over 15 years of experience, he has published in scientific journals and participated in international conferences. He is currently a professor and researcher at the División de Ingeniería y Ciencias Exactas, Universidad Anáhuac Mayab, and a member of SNI, SOMIB, and REI. His main research areas are medical imaging, image biomarkers, and biosignal processing.

Nidiyare Hevia-Montiel received her PhD degree from Paris XI-Orsay University, France. She is currently a Senior Researcher at the Unidad Académica del Instituto de Investigaciones en Matemáticas Aplicadas y en Sistemas del Estado de Yucatán, National Autonomous University of Mexico. Her research interests include computer vision and artificial intelligence applied to biomedical, biological, and environmental applications.

Fernando Arámbula-Cosío is a Lecturer at the Institute of Applied Mathematics and Systems at the Unidad Académica del Instituto de Investigaciones en Matemáticas Aplicadas y en Sistemas del Estado de Yucatán, National Autonomous University of Mexico, working in medical image analysis and computer-assisted surgery since 1997. He has more than 75 papers published in journals and conferences.

Didier Torres-Guzmán earned his Ph.D. in Engineering Sciences from Monterrey Institute of Technology, Mexico, in 2015. With nearly 18 years of professional experience, his work has centered on teaching and research in Advanced Digital Design, Biosignal Processing, and Biomedical Instrumentation. He is the lead inventor of a patent granted in 2018, holds four registered copyrights, and has authored numerous articles in peer-reviewed scientific journals. Currently, Dr. Torres serves as a full-time professor in the Department of Biomedical Systems Engineering at the Faculty of Engineering, National Autonomous University of Mexico (E-mail: didier.torres@unam.mx).